The Astrophysical Journal Letters, 772:L4 (5pp), 2013 July 20 doi:10.1088/2041-8205/772/1/L4

ON THE NEUTRINO NON-DETECTION OF GRB 130427A

Shan Gao, Kazumi Kashiyama, and Peter Mészáros
Department of Physics, Department of Astronomy and Astrophysics, Center for Particle Astrophysics, The Pennsylvania State University, University Park, PA 16802, USA; sxg324@psu.edu, kzk15@psu.edu, pmeszaros@astro.psu.edu
Received 2013 May 29; accepted 2013 June 15; published 2013 July 1

ABSTRACT

The recent gamma-ray burst GRB 130427A has an isotropic electromagnetic energy $E^{\rm iso} \sim 10^{54}$ erg, suggesting an ample supply of target photons for photo-hadronic interactions, which at its low redshift of $z \sim 0.34$ would appear to make it a promising candidate for neutrino detection. However, the IceCube collaboration has reported a null result based on a search during the prompt emission phase. We show that this neutrino non-detection can provide valuable information about this gamma-ray burst's (GRB's) key physical parameters such as the emission radius R_d, the bulk Lorentz factor Γ, and the energy fraction converted into cosmic rays ϵ_p. The results are discussed both in a model-independent way and in the specific scenarios of an internal shock (IS) model, a baryonic photospheric (BPH) model, and a magnetic photospheric (MPH) model. We find that the constraints are most stringent for the MPH model considered, but the constraints on the IS and the BPH models are fairly modest.

Key words: gamma-ray burst: individual (130427A) – neutrinos

Online-only material: color figures

1. INTRODUCTION

Gamma-ray bursts (GRBs) have been proposed as a major source of high-energy cosmic rays, provided that a substantial fraction of protons are accelerated in the inferred shocks or magnetic reconnection regions. However, the underlying mechanism of the prompt gamma-ray emission, the jet structure, and the particle acceleration details remain uncertain. Very high energy neutrinos, however, would be a natural by-product from high-energy protons interacting with other baryons or with photons, suffering little from absorption effect along the propagation path, and providing valuable clues about the presence of cosmic rays. It is expected that if a major fraction of the GRB energy is converted into ultra-high-energy cosmic rays, a detectable neutrino fluence should appear in IceCube (Ahlers et al. 2011). However, the two-year data gathered by the IceCube 40 + 59 string configuration have challenged this scenario by a null result in the search for correlation with hundreds of electromagnetically detected GRBs (Abbasi et al. 2012). Constraints on the conventional IS fireball models have been derived (He et al. 2012) and several alternative models have been discussed (Vurm et al. 2011; Zhang & Yan 2011; Gao et al. 2012).

Recently a superluminous burst, GRB 130427A, was detected simultaneously by five different satellites, with an isotropic equivalent energy of $E^{\rm iso} \sim 10^{54}$ erg in gamma rays at a low redshift of $z \sim 0.34$ (Fan et al. 2013). Disappointingly, a neutrino search for this GRB reported by the IceCube collaboration yielded a null result.[1] Here, we show that this null detection is not surprising and that it provides interesting information about the properties of this GRB, some of which are otherwise difficult to obtain through conventional electromagnetic channels. We discuss the constraints on the physical parameters of this GRB, both (1) using a model-independent procedure patterned after that of Waxman & Bahcall (1997) and Zhang & Kumar (2012; Section 2), and (2) for three specific GRB models (internal shock (IS), baryonic photospheric (BPH), and magnetic photospheric (MPH); Section 3), summarizing our results in Section 4.

[1] http://gcn.gsfc.nasa.gov/gcn3/14520.gcn3

2. MODEL-INDEPENDENT CONSTRAINTS ON THE DISSIPATION RADIUS, BULK LORENTZ FACTOR, AND TOTAL COSMIC-RAY ENERGY

We assume a simple GRB jet model, whose Lorentz factor averaged over the jet cross has a value Γ at the dissipation radius R_d. Generally R_d is model-dependent and is a function of Γ. However, in the interest of generality, in this section we do not specify the underlying models, leaving this for Section 3. Here, the parameters Γ and R_d are treated as two independent variables. At R_d, a fraction of jet total energy $E_{\rm tot}$ (in the form of kinetic energy and a possible toroidal magnetic field energy if the jet is highly magnetized) is dissipated and converted into energy carried by accelerated cosmic-ray protons $\epsilon_p E_{\rm tot}$, turbulent magnetic fields $\epsilon_B E_{\rm tot}$, and high-energy non-thermal electrons $\epsilon_e E_{\rm tot}$ (the latter promptly converting into photons).

For GRB 130427A, the photon spectrum is well fitted by a Band-function spectrum with $dN/dE \propto (E/E_{\gamma b})^{-s}$ in the observer frame, where $s = 0.79$ for $E < E_{\gamma b}$ and $s = 3.06$ for $E_{\gamma b} < E < 10$ MeV, with a spectral break energy $E_{\gamma b} = 1.25$ MeV and a total isotropic equivalent $E_\gamma \sim 1.05 \times 10^{54}$ erg (Fan et al. 2013). For simplicity, in this paper we assume $\epsilon_e = 0.1$, corresponding to a jet total energy, $E_{\rm tot} = 10 E_\gamma$. The value of ϵ_B is uncertain (see, e.g., Lemoine et al. 2013); here we use a value $\epsilon_B = 0.01$. A high magnetic field would suppress the neutrino spectrum at very high energies, since the $\pi^\pm$ and $\mu^\pm$ would have time to cool by synchrotron emission before they decay (see, e.g., Rachen & Meszaros 1998). However, for GRB 130427A, as we show below, the neutrino flux decreases rapidly as the energy increases above the peak, the final expected event rate in IceCube being insensitive to ϵ_B. For the neutrino calculation, we follow the outlines in Waxman & Bahcall (1997) and Zhang & Kumar (2012); see also Zhang & Kumar (2012), Li (2012), He et al. (2012), and Hümmer et al. (2012) for detailed treatments. For this specific GRB, the analytical approximations in this section lead to an error of <30% compared to the

results obtained with the methods in Section 3, for most of the realistic parameters. The cosmic rays are accelerated to a $dN_p/dE \propto E^{-2}$ spectrum up to a maximum energy $E_{p,\max}$ determined either by the Hillas condition or by $t_{\rm dyn} = t_{\rm acc}$ (in the jet frame and converted to the observer frame), whichever is smaller. Here, $t_{\rm dyn} \sim R_d/\Gamma c$ is the dynamical timescale and $t_{\rm acc} \sim o(1) \times E_p/eBc$ is the acceleration timescale in the jet frame. High-energy protons lose energy in the jet frame due to $p\gamma$ interaction, at a rate

$$t_\pi^{-1} \equiv -\frac{d\gamma_p}{\gamma_p dt} = \frac{c}{2\gamma_p^2}\int_{E_{\rm TH}}^{\infty} dE\sigma_{p\gamma}\kappa E \int_{E/2\gamma_p}^{\infty} x^{-2}n(x)dx. \quad (1)$$

The second integral can be solved analytically for the broken power-law photon energy distribution $n(E) = dN_{ph}/dE$, while for the first integral is approximated using the Δ^{1232} resonance, in which, $\sigma_{p\gamma} = \delta(E - E_{pk})5 \times 10^{-28}$ cm^2 where $E_{pk} = 0.3$ GeV is the peak of the $p\gamma$ cross section, $E_{\rm TH} = 0.2$ GeV is the threshold, and $\Delta E = 0.3$ GeV is the width of the resonance measured in the proton rest frame. $\kappa = 0.2$ is the averaged inelasticity of the $p\gamma$ interaction, or $E_p = 5E_\pi$. It is convenient to define the pionization efficiency

$$f_\pi \approx \min\left(1, t_\pi^{-1}/t_{\rm dyn}^{-1}\right), \quad (2)$$

which describes the fraction of energy flowing from parent protons to pions within the dynamical timescale. Of f_π, about 1/2 goes to π^+ and 1/2 to π^0, and neutrinos are produced by the charged pion decay

$$\pi^\pm \rightarrow \mu^\pm + \nu_\mu(\bar{\nu}_\mu) \rightarrow e^\pm + \nu_e(\bar{\nu}_e) + \nu_\mu + \bar{\nu}_\mu. \quad (3)$$

The energy of the charged pion is approximately equally divided among the four leptons, $E_\pi = 4E_\nu$. Due to neutrino oscillations and the large uncertainties in the exact energy and distance of the source, we assume that they arrive at the earth in equal numbers per flavor. Thus, we can express the muon + anti-muon neutrino flux ($\phi \equiv dN/dE$) in the observer frame as

$$\phi_{f_\pi<1}(E) = 4.8 \times 10^{-12} L_{\gamma,53}^2(\epsilon_p/\epsilon_e)(\epsilon_{\gamma b/\rm MeV})(1+z)^2 \Gamma_{300}^{-6} D_{27}^{-2} R_{13}^{-1}(E/E_{\nu b})^{s-3}\ {\rm GeV}^{-1}\ {\rm cm}^{-2} \quad (4)$$

$$\phi_{f_\pi\geqslant 1}(E) = 0.8 \times 10^{-12} L_{\gamma,53}(\epsilon_p/\epsilon_e)(1+z)^3 \Gamma_{300}^{-4} D_{27}^{-2}(E/E_{\nu b})^{-2}\ {\rm GeV}^{-1}\ {\rm cm}^{-2}, \quad (5)$$

where $s = 3.06$ (higher Band index) for $E < E_{\nu b}$ and $s = 0.79$ (lower Band index) for $E > E_{\nu b}$. The pionization efficiency in the above equation is

$$f_\pi = 6.13 L_{\gamma,53} R_{13}^{-1}(E_{\gamma b}/{\rm MeV})\Gamma_{300}^{-2}(1+z)^{-1}(E/E_{\nu b})^{\alpha-1}, \quad (6)$$

with the first neutrino break energy (due to those protons interacting with the $E = E_{\gamma b}$ photons) at

$$E_{\nu b} = 6.33 \times 10^5 (E_{\gamma b}/{\rm MeV})\Gamma_{300}^2(1+z)^{-2}\ {\rm GeV} \quad (7)$$

and a second neutrino break energy (due to synchrotron and inverse Compton cooling by charged pions, assuming Thomson regime for simplicity)[2] at

$$E_{\nu b,2} = 2.12 \times 10^7 L_{\gamma,53}^{-1/2} R_{13}\Gamma_{300}^2(1+z)^{-1} (\epsilon_{B,-1} + \epsilon_{e,-1})^{1/2}\ {\rm GeV}. \quad (8)$$

[2] For energy above this, it is good approximation to treat it as a cutoff for this GRB.

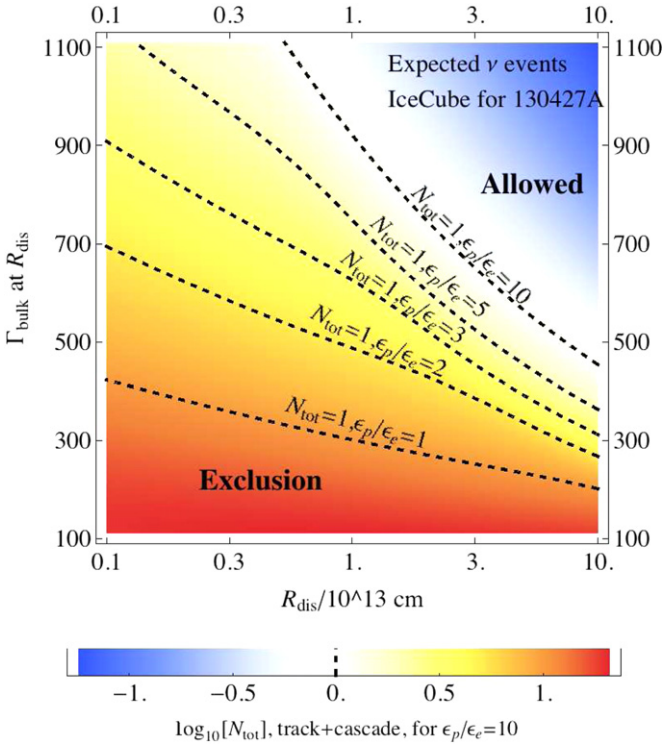

Figure 1. Density plot of the expected number of neutrino events (track+cascade) in IceCube for GRB 130427A on the two-dimensional parameter space of the dissipation radius $R_{13} = R_d/10^{13}$ cm and the bulk Lorentz factor Γ of the jet at this radius. This calculation uses the semi-analytical method similar to Waxman & Bahcall (1997) and Zhang & Kumar (2012) but assuming no specific scenario (e.g., neither an internal shock, nor other model; see Section 2 for details). The blue color (top right region) denotes fewer events while the red (lower regions) denotes more events. The five dashed lines from top to bottom show contours where one event is expected for different proton to electron energy ratios $\epsilon_p/\epsilon_e = 10, 5, 3, 2, 1$. The other two energy partition parameters are taken to be constants, $\epsilon_e = 0.1$ and $\epsilon_B = 0.01$. Based on the null result in the IceCube neutrino search reported in Abbasi et al. (2012), the parameter space below each contours is more likely to be ruled out for the corresponding ϵ_p/ϵ_e.

(A color version of this figure is available in the online journal.)

The model-independent expected number of neutrino events $N_{\rm tot}$, including all types (track and cascade events) and flavors, are shown for this GRB in Figure 1. The neutrino flux ϕ in the observer frame is computed using as input the two free parameters R_d and Γ on a 100 × 100 grid, and this is then integrated with the IceCube effective area profile at the source incident angle $dec = -27^\circ$ to obtain $N_{\rm tot}$, from an energy range $10^2 \leqslant E \leqslant 10^9$ GeV which is sufficiently broad to cover the entire neutrino spectra discussed in this paper. The value of $N_{\rm tot}$ is represented by color. Since $N_{\rm tot} \propto \epsilon_p$ by Equations (4) and (5), we show five contours where $N_{\rm tot} = 1$ for different ϵ_p/ϵ_e values. The allowed region in the $R_d - \Gamma$ parameter space favors a moderately high value of R_d and Γ for small ϵ_p; for high proton to lepton energy ratio, e.g., $\epsilon_p/\epsilon_e = 10$, only large Γ and R_d values are admitted (blue or top-right region of the figure). This is consistent with the nature of the $p\gamma$ interactions and the photon spectrum of this GRB for two reasons: (1) the wind comoving frame photon energy density $u_\gamma = L/4\pi R_d^2\Gamma^2 c$ decreases rapidly with R_d and Γ; a low u_γ suppresses f_π and thus the final neutrino flux. (2) The neutrino break energy, where the neutrino flux contributes most to the final $N_{\rm tot}$ in IceCube, is proportional to Γ^2. A higher $E_{\nu b}$ is associated with a smaller contribution (due to the effective area function and the photon indices for this GRB).

3. CONSTRAINTS ON THE INTERNAL SHOCK, BARYONIC PHOTOSPHERE, AND MAGNETIC PHOTOSPHERIC MODELS

In this section we discuss these three scenarios, labeled IS, BPH, and MPH. After specifying any one of them, R_d is derivable from Γ and the other parameters, and hence one degree of freedom is eliminated from the parameter space. For the IS model, semi-relativistic shocks are formed by the collision of two shells of different velocities. The dissipation radius is estimated as $R_{d,is} \sim \Gamma^2 c\Delta t = 0.27 \times 10^{13}\Gamma^2_{300}\Delta t_{ms}$ cm, where $\Delta t = 10^{-3}\Delta t_{ms}$ s is the variability timescale in milliseconds and Γ is the averaged bulk Lorentz factor of the two shells. For the two photospheric models, the dissipation is assumed to take place at the photosphere where the optical depth for a photon to scatter off an electron is unity $\tau_{\gamma e} = 1$. Depending on whether the jet is dominated by the kinetic energy of the baryons or by the toroidal magnetic energy, the photospheric scenario is either a BPH or an MPH type. For the magnetic type, the fast rotating central engine (a black hole or a magnetar) can lead to a highly magnetized outflow which is initially Poynting-dominated with a sub-dominated baryonic load. If the magnetic field is striped, carrying alternating polarity and the jet is roughly one dimensional, the bulk acceleration of the jet is approximately $\Gamma(r) = (r/r_0)^{1/3}$ until a saturation radius $r_{\rm sat} = r_0\eta^3$, where $r_0 = 10^7 R_7$ cm is the base radius of the jet and $\eta = L_{\rm tot}/\dot{M}c^2$ is the baryon load portion. Around the photosphere region,[3] we assume a major fraction of the jet energy (whether baryonic or magnetic) is dissipated, leading to proton acceleration, resulting in a proton spectrum $dN_p/dE \propto E^{-2}$ similar to that expected from a *Fermi* process, as is the case with the IS model; e.g., see Murase (2008), Wang & Dai (2009), and Drury (2012). For most reasonable parameters, in the magnetic MPH model we have $\Gamma \lesssim \eta$ where the jet is still in the acceleration phase at the dissipation radius. On the other hand, for the BPH and IS models, the dissipation radius almost always occurs outside the saturation radius, namely $\Gamma = \eta$. The determination of R_d is more complicated for photosphere models than it is for the IS models, due to many factors (e.g., (Vurm et al. 2011; Uzdensky & McKinney 2011).) For example, the jet may be contaminated by the electron positron pairs which will substantially increase $\tau_{\gamma e}$ and $R_{\rm phot}$. A more realistic consideration should also include the fact that the dissipation can start from the sub-photosphere all the way out, until the jet is saturated. The magnetic field configuration is also complex (e.g., the geometry of the layers, the reconnection rates etc.) which will eventually affect the proton and neutrino spectrum. Although a multi-zone simulation is beyond the scope of this paper, it would be desirable in order to increase the precision of the neutrino spectrum.

In this section, we have used a calculation scheme similar to that in Gao et al. (2012).[4] We make the same assumptions suitable for a one-zone calculation, but the consideration on the micro-processes is here more complete, compared to that of Section 2, and is based on a numerical code. The pionization efficiency is obtained by calculating all the leading order processes, e.g., $p\gamma$ (Delta resonance and multi-pion productions), Bethe–Heitler, pp, synchrotron, inverse Compton, and adiabatic losses. The cooling of the secondary charged particles via synchrotron and inverse Compton, and the energy distribution functions for the neutrinos from pion and muon decay are also included. The expected neutrino events detectable in IceCube are plotted in Figures 2–4 for the three models separately. The asymptotic Lorentz factor η (instead of Γ at the dissipation radius) and the ratio of accelerated protons to electrons ϵ_p/ϵ_e are the two input free parameters. The calculation is performed on a 50×60 grid for this parameter space for each model. The resultant neutrino event number, N_μ (tracks only) and $N_{\rm tot}$ (track+cascade), are represented by colors. We also show the contours in each figure where $N_\mu = 1$ and $N_{\rm tot} = 1$.

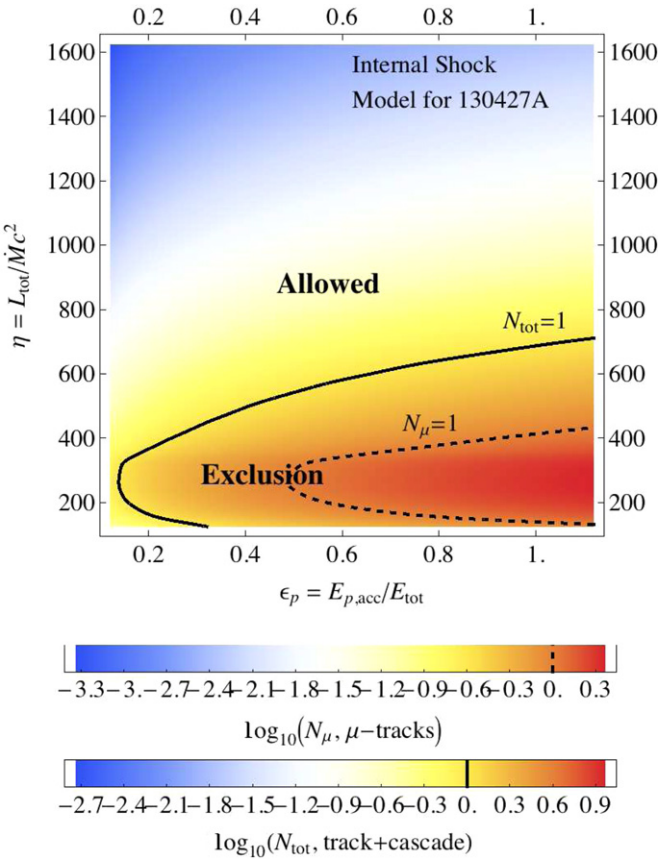

Figure 2. Density plot of expected neutrino event number in IceCube based on the internal shock model for GRB 130427A. The total number $N_{\rm tot}$ (muons + cascades) and N_μ (muons only) are calculated in the two-dimensional parameter space η and ϵ_p. Here, R_d is the internal shock radius for a 1 ms variability timescale (see Section 3). The value of N is represented the by color; however, for $N_{\rm tot}$ and N_μ the value of the color coding is different—see the upper and lower legends. The contours where $N_{\rm tot} = 1$ and $N_\mu = 1$ are also shown by solid and dashed lines, respectively. The other energy fractions are taken as constants, $\epsilon_e = 0.1$ and $\epsilon_B = 0.01$. The IceCube null result favors the yellow and blue regions, e.g., a high η.

(A color version of this figure is available in the online journal.)

Constraints on IS models (Figure 2). Here we have used a variability timescale $\Delta t = 1$ ms. This corresponds to a minimal dissipation radius $R_d \sim 2.7 \times 10^{13}\Gamma^2_{300}$ cm which is optimally advantageous for neutrino production. A higher value of Δt would increase R_d and decrease f_π and ϕ from those shown in Figure 1. Thus, the constraints should be considered looser when using a higher value of Δt. The results suggest that ϵ_p/ϵ_e values from 1 to 10 can all be admitted, but for $\epsilon_p/\epsilon_e > 5$, $\Gamma > 600$ is required in order not to violate the IceCube null result. We note also that $N_{\rm tot}$ and N_μ increase when $\eta = \Gamma$ is lowered, but their values saturate at about $\eta = 300$ and then

[3] While in the ICMART model by Zhang & Yan (2011), the magnetic dissipation is determined by the variability timescale, which resembles the internal shock model.

[4] The code is updated to a parallel version to allow the fast computation of a large region parameter space for this paper.

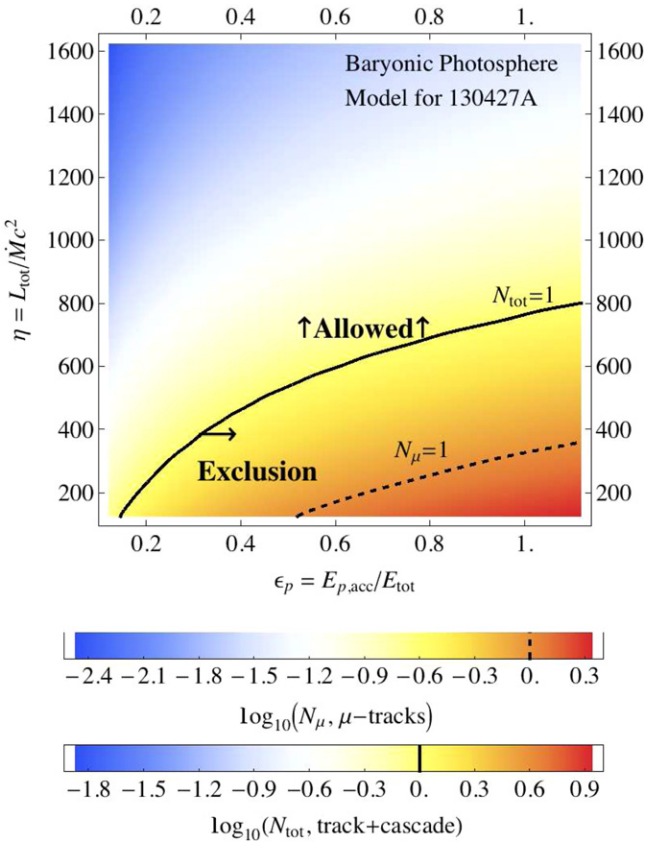

Figure 3. Expected neutrino event number in IceCube based on the baryonic photospheric model for GRB 130427A. The conventions are the same as those in Figure 2. A high η (or Γ) is favored by the null result in IceCube.

(A color version of this figure is available in the online journal.)

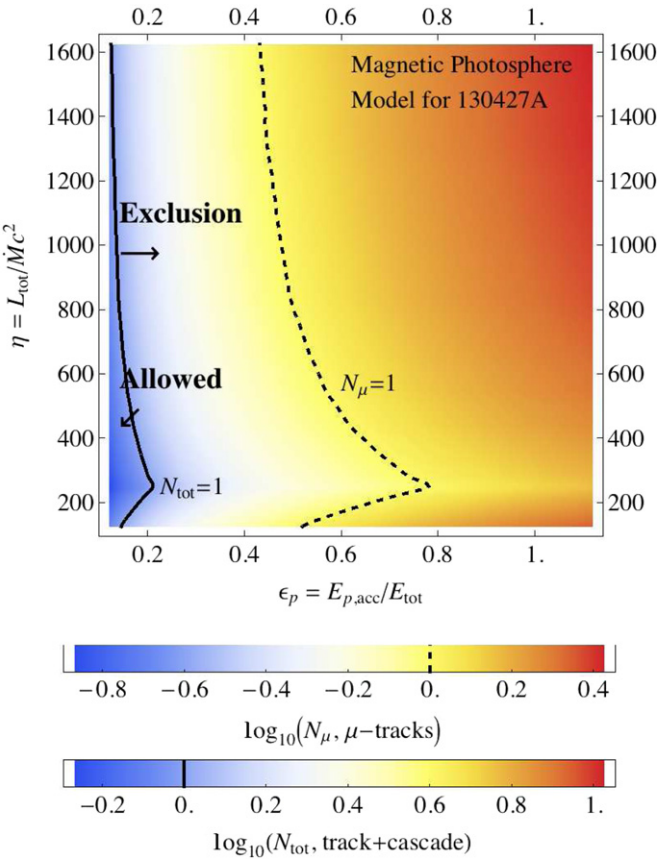

Figure 4. Expected neutrino event number in IceCube based on the magnetic photospheric model for GRB 130427A. The conventions are the same as those in Figure 2. The result is insensitive to η (see Section 3 for an explanation). The null result in IceCube favors the region where $\epsilon_p < 0.1 \sim 0.2$, roughly independent of η or Γ.

(A color version of this figure is available in the online journal.)

decrease when $\eta < 300$. For $\eta \lesssim 300$, f_π reaches unity and protons lose almost all their energy to pions. A smaller radius is associated with a higher energy density u_B and u_γ, which causes the charged pions and muons to cool faster before they decay to produce neutrinos. A smaller Γ value gives a smaller $E_{\nu b}$ value, for which IceCube has a smaller effective area.

Constraints on the BPH model (Figure 3). The photospheric radius is estimated as $R_{\rm phot} \approx \sigma_T L_{\rm tot}/4\pi\Gamma^3 m_p c^3$. The result coincidentally resembles the IS model with $\Delta t = 1$ ms. However, at low Γ values, $R_{\rm phot}$ rapidly increases, which is different from the $R_d \propto \Gamma^2$ behavior of the IS model. On the contrary, only at high-η values does the magnetic field begin to cool the charged secondaries significantly, leading to a suppressed neutrino spectrum.

Constraints on the MPH model (Figure 4). The most interesting constraints are obtained for the MPH model. Due to the nature of the magnetic jet, the photosphere, if one neglects the effects of $e^\pm$ formation (Veres & Mészáros 2012), should occur in the acceleration phase for the likely parameter values. Even if the jet is initially loaded with a small amount of baryons (a high-η value), Γ at $R_{\rm phot}$ is roughly a constant value $150 \leqslant \Gamma \leqslant 200$ for most η choices. This fact is also revealed in Figure 4 by the contours being almost parallel to the Γ-axis. The MPH radius is larger than the R_d computed for the IS model with $\Delta t = 1$ ms, but it is not large enough to suppress f_π much below unity. The secondaries suffer somewhat less cooling from synchrotron and IC than in the IS case considered. A somewhat lower bulk Lorentz factor[5] is advantageous for neutrino production. Therefore, the MPH model generally has an equal or higher neutrino efficiency than the IS and BPH models. Although the result is insensitive to η, a relatively stringent constraint on $\epsilon_p/\epsilon_e \leqslant 1 \sim 2$ is obtained for this burst, independent of η or Γ. For very low values of η, there is also a "saturation effect" for reasons similar as in the IS case.

[5] However, $E_{\nu b}$ is also lower, which decreases the event number in IceCube.

4. DISCUSSION

We have discussed the implications of the non-detection by IceCube in the gamma-ray burst GRB130427A. Using the results of the electromagnetic observations of this burst, we have analyzed the implications of this neutrino null result for constraining the physical parameters of this burst. Using first a simplified analysis which is independent of specific GRB models, we find that the null result implies a simple inverse relationship between the bulk Lorentz factor Γ at the dissipation radius R_d and this radius, as a function of the relativistic proton to electron ratio ϵ_p/ϵ_e (Figure 1), which suggests values of $\Gamma \gtrsim 500$ and $R_d \gtrsim 10^{14}$ cm. We then performed more detailed numerical calculations for three different specific GRB models, the IS, BPH, and MPH models. We find that the IS model (Figure 2) with the shortest variability time and the highest neutrino luminosity is able to comply with the null-result constraint if its bulk Lorentz factor $\Gamma = \eta \gtrsim$

400–600, depending on ϵ_p/ϵ_e, a fairly modest constraint. Longer variability times only weaken the constraint. For the baryonic photosphere BPH model (Figure 3) the constraint for compliance is comparable, $\Gamma = \eta \gtrsim$ 600–700 depending on ϵ_p/ϵ_e. The most restrictive constraint is for the magnetic photosphere MPH model of Figure 4. Here it is found that, for this burst GRB130427A, the null result implies an allowed value of $\epsilon_p/\epsilon_e \lesssim$ 1–2, almost independently of the asymptotic bulk Lorentz factor η. More careful calculations of all three types of models will clearly be required for reaching firm conclusions, but based on the above considerations, the generic IS and BPH models are not significantly constrained by the lack of observed neutrinos.

We are grateful to the useful comments by the anonymous referee, and NASA NNX13AH50G and JSPS for partial support.

REFERENCES

Abbasi, R., Abdou, Y., Abu-Zayyad, T., et al. 2012, Natur, 484, 351
Ahlers, M., Gonzalez-Garcia, M. C., & Halzen, F. 2011, APh, 35, 87
Drury, L. O. 2012, MNRAS, 422, 2474
Fan, Y.-Z., Tam, P. H. T., Zhang, F.-W., et al. 2013, arXiv:1305.1261
Gao, S., Asano, K., & Meszaros, P. 2012, JCAP, 11, 58
He, H.-N., Liu, R.-Y., Wang, X.-Y., et al. 2012, ApJ, 752, 29
Hümmer, S., Baerwald, P., & Winter, W. 2012, PhRvL, 108, 231101
Lemoine, M., Li, Z., & Wang, X.-Y. 2013, arXiv:1305.3689
Li, Z. 2012, PhRvD, 85, 027301
Murase, K. 2008, PhRvD, 78, 101302
Rachen, J. P., & Meszaros, P. 1998, PhRvD, 58, 123005
Uzdensky, D. A., & McKinney, J. C. 2011, PhPl, 18, 042105
Veres, P., & Mészáros, P. 2012, ApJ, 755, 12
Vurm, I., Beloborodov, A. M., & Poutanen, J. 2011, ApJ, 738, 77
Wang, X., & Dai, Z. 2009, ApJ, 691, 67
Waxman, E., & Bahcall, J. 1997, PhRvL, 78, 2292
Zhang, B., & Kumar, P. 2012, PhRvL, 110, 121101
Zhang, B., & Yan, H. 2011, ApJ, 726, 90